RSC Advances

PAPER

View Article Online
View Journal | View Issue

Check for updates

Cite this: *RSC Adv.*, 2026, **16**, 11700

Effect of sulfidated nanoscale zero-valent iron-activated periodate on bacterial inactivation and conjugative gene transfer

Li Liang[ab] and Weiying Li *[b]

Abuse of antibiotics can cause a serious global issue of antibiotic resistance (AR). This research studied the efficiency of sulfidated nanoscale zero-valent iron (S-nZVI)-activated periodate toward the inactivation of antibiotic-resistant bacteria (ARB) and the conjugative transfer of antibiotic resistance genes (ARGs), with *E. coli* strains HB101 (carrying the RP4 plasmid) and NK5449 as the donor and recipient, respectively. In comparison to the control group (without treatment with S-nZVI/PI), the ARG conjugative transfer frequency within 24 h decreased from 6.3×10^{-4} to 6.6×10^{-5} after treatment with the S-nZVI/PI system (S-nZVI = 50 mg L^{-1}, and PI = 1.0 mM) for 40 min. The S-nZVI/PI system functioned as an inhibitor of conjugative transfer for ARGs, which was attributed to the inhibition of the synthesis of the driving-energy adenosine triphosphate (ATP) and prevention of gene expression regarding contact and pairing (*traF*), assembly of a transmembrane DNA transport channel (*trbA*), transfer of ssDNA from donor bacteria to recipient bacteria (*traG*), and global regulation (*traJ*, *korA*, and *korB*). Increasing the dosages of S-nZVI and PI could increase the sterilization of the donor and recipient, while the conjugative transfer of ARGs was less influenced by the S-nZVI and PI dosages. The decline in the initial concentration of the donor and recipient could increase the bactericidal efficiency and decrease the ARG conjugative transfer frequency. HCO_3^- and HA existing in the S-nZVI/PI system exhibited inhibitory roles against both bacterial inactivation and ARGs conjugative transfer. The findings of this study could provide a valid alternative for remediating environments contaminated with ARB and controlling the dissemination of AR.

Received 30th October 2025
Accepted 11th February 2026

DOI: 10.1039/d5ra08354k

rsc.li/rsc-advances

Open Access Article. Published on 02 March 2026. Downloaded on 5/24/2026 3:56:50 AM.
This article is licensed under a Creative Commons Attribution-NonCommercial 3.0 Unported Licence.

1. Introduction

The use of antibiotics is very common in disease treatment, agriculture, and livestock farming.[1–5] Ingested antibiotics cannot be fully metabolized by humans and animals. About 30–90% of antibiotics are excreted to the environment through feces and urine,[1] which pose selective pressure on bacteria, thereby promoting the development of antibiotic-resistant bacteria (ARB) and the proliferation of antibiotic resistance genes (ARGs) and further causing a serious global crisis called antibiotic resistance (AR).[6]

Horizontal transfer, which is mediated by mobile genetic elements (MGEs), such as integrons, transposons, and plasmids,[7] and vertical transfer of ARGs,[8] can derive new ARBs and accelerate AR spread. Horizontal transfer is the dominant form that increases the risk of ARGs transmission. The types of horizontal transfer include conjugative, transformative, and transductive mechanisms.[9] Notably, conjugation serves as the main channel to enable the dissemination of ARGs according to the direct contact of donor and recipient bacteria.[10] It has been reported that the pollution of AR has a serious impact on human health, such as drug inactivation.[11] Therefore, it is urgent to investigate a valid technology that can not only enable the inactivation of ARB but also suppress the ARGs horizontal transfer.

Traditional disinfection methods (such as chlorine, ultraviolet, and ozone) and advanced oxidation processes (AOPs) (such as photocatalysis, Fenton, and activated persulfate (PS) or periodate (PI)) were used to enable the inactivation of ARB and the removal of ARGs.[12–17] However, traditional disinfection methods were negligible in the removal of ARGs and even promoted the horizontal transfer of ARGs under sub-inhibitory concentrations.[18] For example, when the concentration of chlorine was 4 mg Cl_2/L, the conjugative transfer frequency of ARGs increased by 2–5 fold within 10 min relative to the untreated group.[19] Compared with traditional disinfection methods, AOPs exhibited superior performance in eliminating

[a]*Key Laboratory of Water Security and Water Environment Protection in Plateau Intersection, Ministry of Education, Key Laboratory of Bioelectrochemistry and Environmental Analysis of Gansu Province, College of Chemistry and Chemical Engineering, Northwest Normal University, Lanzhou 730070, PR China*

[b]*State Key Laboratory of Pollution Control and Resource Reuse, Key Laboratory of Yangtze River Water Environment of the Ministry of Education, College of Environmental Science and Engineering, Tongji University, Shanghai, 200092, PR China. E-mail: 123lwyktz@tongji.edu.cn*

© 2026 The Author(s). Published by the Royal Society of Chemistry

Open Access Article. Published on 02 March 2026. Downloaded on 5/24/2026 3:56:50 AM. This article is licensed under a Creative Commons Attribution-NonCommercial 3.0 Unported Licence.

both ARB and ARGs and controlling the dissemination of ARGs owing to the reactive oxygen species (ROS) formation.[20]

Compared to other oxidizing agents (such as H_2O_2, peroxymonosulfate (PMS), and peroxydisulfate (PDS)), PI-driven AOPs have garnered considerable interest due to their exceptional efficacy in removing various pollutants, including pharmaceuticals, dyes, phenolic compounds, and bacteria.[21–23] It was found that the degradation rate of sulfadiazine and the inactivation of ARB by PI-based AOP were significantly higher than those of H_2O_2, PMS, and PDS-based AOPs under identical experimental conditions.[24,25] Moreover, no toxic iodinated compounds (*i.e.* hypoiodous acid and I_2) were generated in PI-driven AOPs.[26] With respect to bacteria disinfection by PI-driven AOPs, the activation methods of PI included simulated solar,[27,28] hydroxylamine,[29] and iron-based materials (such as pyrite and sulfidated nanoscale zero-valent iron (S-nZVI)).[25,30] Sun *et al.* found that the combination of PI and hydroxylamine could inactivate 10^6 CFU mL^{-1} *E. coli* and *S. aureus* completely within 2 min. However, the reaction system might generate greenhouse gas N_2O.[29] Compared to simulated solar, PI activation by materials based on iron could shorten the inactivation time of ARB. For instance, the full inactivation of 10^7 CFU mL^{-1} *E. coli* by the pyrite-activated PI was 20 min, which was two times shorter than that of the simulated solar-activated PI,[28,30] thus decreasing the hydraulic residence time and reducing infrastructure and operational costs in practice. S-nZVI, as one of the most versatile iron-based nanomaterials, was extensively used to remove a variety of contaminants due to its high reactivity, selectivity, and low cost.[31–35] Our previous study found that S-nZVI could also be used to activate PI to achieve the efficient elimination of ARB and its carried ARGs by the generated ROS $HO^{\bullet}$ and $O_2^{\bullet-}$ to destroy the morphology and intracellular enzyme system.[25] However, the treatment efficiency of the S-nZVI/PI system for the control of ARGs transfer is still unknown, which warrants further research.

Accordingly, *E. coli* HB101, harboring the RP4 plasmid containing ARGs (including *aphA*, *tetA*, and *tnpA*), and *E. coli* NK5449 were employed as the donor and recipient strains, respectively. The study aims to (1) evaluate the influence of key operational parameters, including PI and S-nZVI dosage, initial bacterial concentrations, and the presence of interfering substances (*e.g.*, HCO_3^-, NO_3^-, and humic acid (HA)), on the efficacy of inactivating both donor and recipient bacteria and the conjugative transfer frequency of ARGs and (2) clarify the mechanism for suppressing conjugative transfer of ARGs. These findings are expected to offer a viable strategy for mitigating the dissemination of AR.

2. Materials and methods

2.1. Chemical reagents

Sodium periodate ($NaIO_4$, ≥ 99.5%) and sodium sulfide nonahydrate ($Na_2S·9H_2O$, ≥ 98.0%) were obtained from Aladdin Reagent Co., Ltd (Shanghai, China). Luria-Bertani (LB) nutrient agar and LB broth were acquired from Qingdao Hope Bio-Technology Co., Ltd (Qingdao, China). Ampicillin trihydrate ($C_{16}H_{19}N_3O_4S·3H_2O$), rifampicin ($C_{43}H_{58}N_4O_{12}$), and kanamycin sulfate ($C_{18}H_{36}N_4O_{11}H_2SO_4$) were supplied by Beijing Solarbio Science and Technology Co., Ltd (Beijing, China). Tetracycline hydrochloride ($C_{22}H_{24}N_2O_8·HCl$) was provided by Sangon Biotech Co., Ltd (Shanghai, China). Iron trichloride hexahydrate ($FeCl_3·6H_2O$, ≥ 99.0%) was sourced from Sinopharm Chemical Reagent Co., Ltd (Shanghai, China). All reagents were utilized without further purification.

2.2. Synthesis of S-nZVI

S-nZVI was prepared following the procedure described by Liang *et al.*[36]

2.3. Culture of *E. coli* strains HB101 and NK5449

E. coli HB101 was cultured according to a previous method.[25] Briefly, a single colony was inoculated into 100 mL of LB broth containing kanamycin (80 mg L^{-1}), ampicillin (60 mg L^{-1}), and tetracycline (50 mg L^{-1}) and incubated at 37 °C for 12 h under constant shaking (180 rpm). The culturing of *E. coli* NK5449 was similar to that of *E. coli* HB101, in addition to replacing antibiotics with 160 mg L^{-1} rifampicin. The incubated *E. coli* strains HB101 and NK5449 were separately collected into centrifuge tubes and then washed three times with 0.9% saline solution. After that, a certain amount of 0.9% saline solution was employed to resuspend *E. coli* strains HB101 and NK5449 to prepare their stock solution with a concentration of *ca.* 10^9 CFU mL^{-1}.

2.4. Inactivation of *E. coli* strains HB101 and NK5449

Disinfection experiments were conducted in a series of 50 mL Erlenmeyer flasks. Typically, in the disinfection experiments, a quantity of *E. coli* strains HB101 and NK5449 stock solution was added into an Erlenmeyer flask; then, PI and S-nZVI were injected into the disinfection system to begin the reaction. The target concentrations of mixed ARB, PI, and S-nZVI were 10^8 CFU mL^{-1}, 1.0 mM, and 50 mg L^{-1}, respectively. The reaction system was placed in a shaker (25 °C, 250 rpm) and covered with aluminum foil to prevent the light-induced activation of PI. A control experiment (without the S-nZVI/PI addition) was performed to further elucidate S-nZVI/PI efficacy. At predetermined time points, 1.0 mL of mixed bacteria solution was sampled from the reaction mixture and quenched by 20 μL $Na_2S_2O_3$ (1.0 M). Subsequently, the bacterial solution was diluted according to the 10-fold volume dilution method with a 0.9% saline solution. After that, two parts of the 100 μL diluted bacterial solution were evenly coated on the cultivation medium of the donor and recipient strains. All the cultivation media were placed into an incubator (37 °C, 24 h) to enumerate the number of viable cells of *E. coli* strains HB101 and NK5449. The *E. coli* HB101 cultivation medium contained kanamycin (80 mg L^{-1}), ampicillin (60 mg L^{-1}), and tetracycline (50 mg L^{-1}). The *E. coli* NK5449 cultivation medium contained rifampicin (160 mg L^{-1}). The drug sensitivity experiment demonstrated that the cultivation media of both bacteria had specificity; for example, *E. coli* NK5449 could not be grown in the *E. coli* HB101 corresponding cultivation medium and *vice versa*.

Open Access Article. Published on 02 March 2026. Downloaded on 5/24/2026 3:56:50 AM. This article is licensed under a Creative Commons Attribution-NonCommercial 3.0 Unported Licence.

In addition, the effects of the dosages of PI (0.8, 1.0, and 1.2 mM) and S-nZVI (25, 50, and 75 mg L^{-1}), the initial concentrations of donor and recipient (10^6, 10^7, and 10^8 CFU mL^{-1}), and interfering substances (HCO_3^-, NO_3^-, and HA) on the inactivation of *E. coli* HB101 and NK5449 were investigated. In order to guarantee the accuracy of the data, all experiments were replicated three times, and the results were shown as mean values ± standard deviation (SD). Statistical analysis of the data was performed using SPSS software.

2.5. Conjugative transfer of ARGs

Horizontal gene transfer mediated by conjugation under different reaction conditions was conducted after the disinfection experiments. The detailed operation procedures were that 1 mL $Na_2S_2O_3$ (1.0 M) was added into the reaction Erlenmeyer flasks of disinfection reaction to consume the ROS generated in the S-nZVI/PI system. Then, the reaction system was placed on the shaker at 25 °C and 180 rpm to initiate the spread of ARGs through conjugation. The reaction bacteria solution was sampled at 3, 6, 12, and 24 h to count the numbers of *E. coli* strains HB101 and NK5449, and transconjugant using the 10 times volume dilution method, as discussed in subsection 2.4. The cultivation media of *E. coli* strains HB101 and NK5449 were the same as those applied in subsection 2.4. The cultivation medium of the transconjugant consisted of kanamycin (80 mg L^{-1}), ampicillin (60 mg L^{-1}), tetracycline (50 mg L^{-1}), and rifampicin (160 mg L^{-1}). The frequency of ARGs conjugative transfer was quantified according to eqn (1):

$$\text{Conjugative transfer frequency of ARGs} = \text{number of transconjugant/number of recipient ARB (}\textit{E. coli}\text{ NK5449).} \quad (1)$$

2.6. Analytical methods

2.6.1. Detection of adenosine triphosphate (ATP). The content of ATP was detected following the manual of the ATP test kit (Solarbio, BC0300). The detailed protocol was that 1 mL of bacteria solution was treated by ultrasonic processing; then, the corresponding assay reagents were added into the 100 μL ultrasonically treated sample solution and quantified using the microplate reader at a wavelength of 240 nm.

2.6.2. Detection of lactate dehydrogenase (LDH). The LDH can be used to reflect the impairment of the cell membrane. The detection of LDH was performed using the instrument of the manual of the LDH test kit (Solarbio, BC0685). In brief, 1 mL of bacterial solution was treated with ultrasonic processing. 10 μL treated solution was fully mixed with the reagents of LDH detection. The absorbance of the above mixture was quantified at 450 nm using a microplate reader.

2.6.3. Quantification of intracellular *ROS*. Intracellular ROS generation was monitored by applying a reactive oxygen species assay kit (Solarbio, CA1410). The detection of ROS was performed by adding 1 mL 10 μmol L^{-1} 2′,7′-dichlorofluorescin diacetate (DCFH-DA) fluorescent probe into 1 mL bacterial solution and then incubating at 37 °C for 20 min to ensure the complete mixing of the DCFH-DA and bacteria. After that, the mixture was centrifuged at 37 °C and 10000 rpm for 1 min and rinsed thrice with PBS to remove the DCFH-DA that could not enter the cell. Finally, fluorescence intensity was recorded by applying a microplate reader with wavelengths set at 488 nm (excitation) and 525 nm (emission).

2.6.4. Detection of functional genes. (1) Extraction of RNA: the RNA of the mixture of *E. coli* strains HB101 and NK5449 was extracted by applying the Total RNA Extraction Kit (Solarbio, R1200).

(2) Reverse transcription of RNA: the FastKing RT Kit (Tiangen Biotech, KR116) was used to reverse-transcribe RNA into DNA.

(3) Relative abundance of each functional gene: 2 μL DNA template, TB green premix, Ex Taq II reagents, forward and reverse primers, and sterilized water were added into a PCR 8-strip tube. Then, a real-time quantitative polymerase chain reaction (qPCR, 7500 Real-Time PCR System, Thermo Fisher, USA) was utilized to obtain the CT value of each functional gene. The designed forward and reverse primer sequences of each functional gene are displayed in Table S1. qPCR was performed for 40 cycles, as specified below: 30 s of initial denaturation at 95 °C, followed by 5 s at 95 °C and 34 s at 60 °C for each cycle. The relative abundance of each functional gene was calculated using the $2^{-\Delta C}{}_t$ method.[37] ΔC_t was the difference between the C_t of functional genes and the internal reference 16S rRNA. Compared with the control group (without S-nZVI/PI treatment), the fold change in the expression of each functional gene after S-nZVI/PI treatment was calculated using eqn (2). The $\Delta\Delta C_t$ in eqn (2) is the difference between the treatment and control groups:

$$\text{Fold change} = 2^{-\Delta\Delta C_t} \quad (2)$$

3. Results and discussion

3.1. Influence of different factors on the inactivation of *E. coli* strains HB101 and NK5449 and the conjugative transfer of ARGs

3.1.1. Influence of PI dosage. Fig. 1 illustrates the influence of PI dosage on inactivating *E. coli* strains HB101 and NK5449 by applying the S-nZVI/PI treatment system. The inactivation performance for both strains exhibited a positive correlation with the PI dosage. Specifically, as the PI concentration increased from 0.8 to 1.2 mM, the bactericidal efficiency of *E. coli* HB101 and *E. coli* NK5449 increased from 1.8 and 1.1 $\log_{10}$ to 4.5 and 2.4 $\log_{10}$ CFU mL^{-1} after 40 min of treatment, respectively. These results clearly indicate that *E. coli* HB101 was significantly more susceptible to the S-nZVI/PI treatment than that of *E. coli* NK5449 ($p < 0.05$).

The variation in the number of *E. coli* HB101, *E. coli* NK5449, and transconjugant as mating times under different PI dosages is depicted in Fig. S1. When the mating time was 3 h, transconjugant was detected in both the control group (without treatment by S-nZVI/PI) and S-nZVI/PI system (at the 0.8 mM PI dosage), and the transconjugant numbers were 4.8 and 1.2 $\log_{10}$ CFU mL^{-1} in the control group and S-nZVI/PI system,

 © 2026 The Author(s). Published by the Royal Society of Chemistry

Open Access Article. Published on 02 March 2026. Downloaded on 5/24/2026 3:56:50 AM.
This article is licensed under a Creative Commons Attribution-NonCommercial 3.0 Unported Licence.

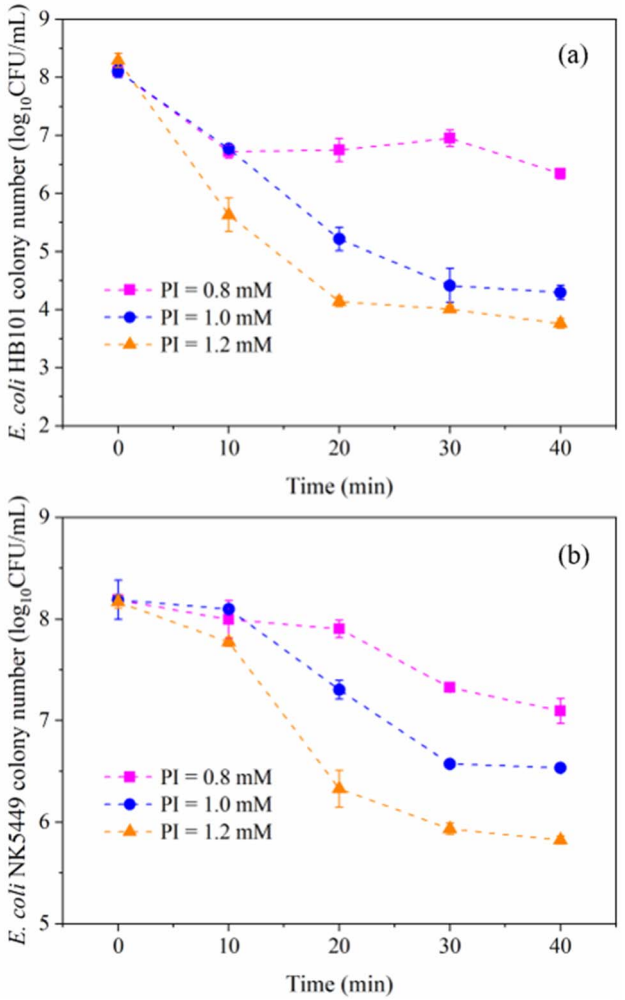

Fig. 1 Inactivation of (a) donor and (b) recipient as a function of the PI dosage. (Experimental conditions: $pH_0 = 6.8$, bacterial concentrations of 10^8 CFU mL^{-1} for both donor and recipient, [S-nZVI] = 50 mg L^{-1}, and the experiments were replicated three times with SD as the error bar).

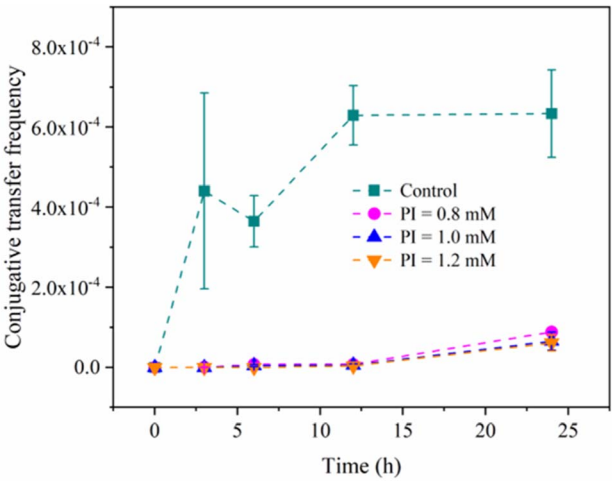

Fig. 2 Effect of PI dosage on the ARGs conjugative transfer frequency. (Experimental conditions: $pH_0 = 6.8$, bacterial concentrations of 10^8 CFU mL^{-1} for both donor and recipient, [S-nZVI] = 50 mg L^{-1}, and the experiments were replicated three times with SD as the error bar).

respectively (Fig. S1a). As the mating time increased to 24 h, transconjugants were observed in all investigated groups (including control and PI dosages of 0.8, 1.0, and 1.2 mM) with numbers of 5.0, 3.6, 2.9, and 2.7 $\log_{10}$ CFU mL^{-1}, respectively (Fig. S1d). Compared to the control group, the S-nZVI/PI system could inhibit the horizontal transfer of the RP4 plasmid between donor and recipient bacteria ($p < 0.05$), and the inhibitory effect increased as PI dosage increased ($p < 0.05$). Moreover, with an increase in mating time, the activity of *E. coli* strains HB101 and NK5449 recovered. After 24 h contact, the numbers of *E. coli* HB101 were 6.0, 6.0, and 5.5 $\log_{10}$ CFU mL^{-1}, and 7.7, 7.1, and 6.9 $\log_{10}$ CFU mL^{-1} for *E. coli* NK5449 at PI dosages of 0.8, 1.0, and 1.2 mM, respectively (Fig. S1d). The recovery of *E. coli* strains HB101 and NK5449 activity during mating time might be the dominant reason for the generation of transconjugants.

The variation in the ARGs conjugation transfer frequency as the mating time at different PI dosages is shown in Fig. 2. Under the same PI dosage, the conjugative transfer frequency between the donor *E. coli* HB101 and the recipient *E. coli* NK5449 increased as mating time increased. When PI dosages were 0, 0.8, 1.0, and 1.2 mM, after 24 h conjugative transfer, the conjugative transfer frequencies of ARGs were 6.3×10^{-4}, 8.9×10^{-5}, 6.6×10^{-5}, and 6.1×10^{-5}, respectively, indicating that the treatment of S-nZVI/PI could significantly inhibit the conjugative transfer of plasmid RP4 in *E. coli* HB101 to *E. coli* NK5449 ($p < 0.05$).

3.1.2. Influence of S-nZVI dosage. As depicted in Fig. 3, the inactivation of *E. coli* strains HB101 and NK5449 exhibited a dose-dependent response to S-nZVI. After treatment with the S-nZVI/PI system for 40 min, *E. coli* strains HB101 and NK5449 were inactivated *ca.* 3.2 and 1.5 $\log_{10}$ CFU mL^{-1}, respectively, at an S-nZVI dosage of 25 mg L^{-1}. When the S-nZVI dosage increased to 75 mg L^{-1}, the inactivation of *E. coli* strains HB101 and NK5449 by the S-nZVI/PI system was enhanced to 4.1 and 1.9 $\log_{10}$ CFU mL^{-1}, respectively.

As shown in Fig. S2, part of the *E. coli* strains HB101 and NK5449 would repair their lost cultivability after the conjugative transfer experiment, thus resulting in the generation of transconjugants. It was found that the numbers of transconjugants were 5.0, 3.6, 2.9, and 3.0 $\log_{10}$ CFU mL^{-1} within 24 h of conjugative transfer when the dosages of S-nZVI were 0, 25, 50, and 75 mg L^{-1} (Fig. S2d).

The change in the conjugative transfer frequency of ARGs with different S-nZVI dosages is shown in Fig. 4. The conjugative transfer frequency of the ARGs increased with mating time increasing. Following 24 h of conjugative transfer at S-nZVI dosages of 0, 25, 50, and 75 mg L^{-1}, the conjugative transfer frequencies of ARGs were 6.3×10^{-4}, 9.2×10^{-5}, 6.6×10^{-5}, and 5.4×10^{-5}, respectively. Although the treatment of S-nZVI/PI could lower the conjugation-mediated ARGs transfer, there was no significant difference between different S-nZVI dosages (25, 50, and 75 mg L^{-1}) ($p > 0.05$).

3.1.3. Influence of initial concentrations of *E. coli* strains HB101 and NK5449. The effects of initial bacterial

Open Access Article. Published on 02 March 2026. Downloaded on 5/24/2026 3:56:50 AM.
This article is licensed under a Creative Commons Attribution-NonCommercial 3.0 Unported Licence.

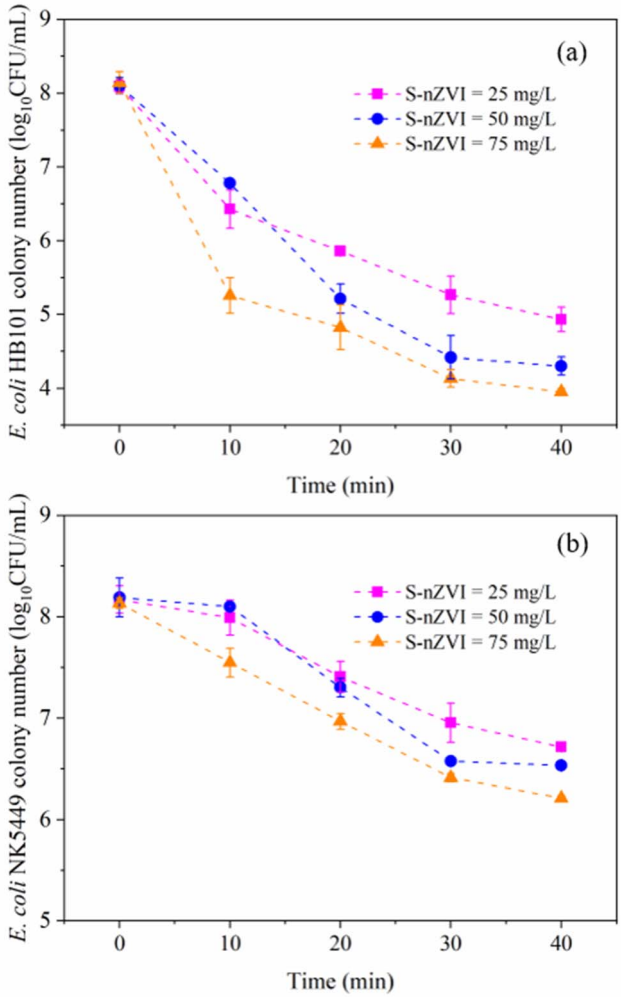

Fig. 3 Inactivation of (a) donor and (b) recipient as a function of the S-nZVI dosage. (Experimental conditions: $pH_0 = 6.8$, bacterial concentrations of 10^8 CFU mL^{-1} for both donor and recipient, [PI] = 1.0 mM, and the experiments were replicated three times with SD as the error bar).

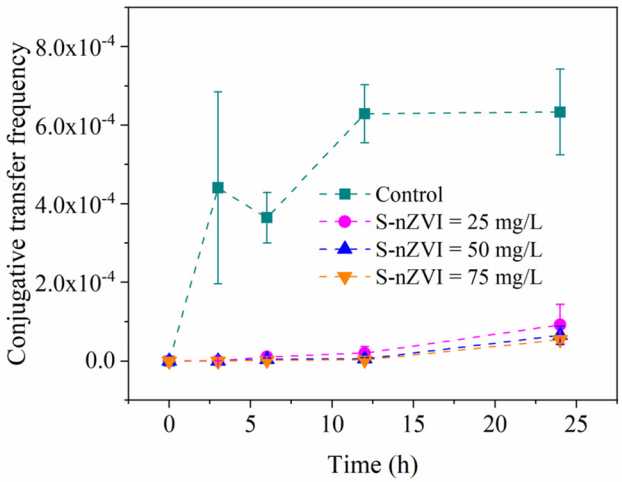

Fig. 4 Effect of S-nZVI dosage on the ARGs conjugative transfer frequency. (Experimental conditions: $pH_0 = 6.8$, bacterial concentrations of 10^8 CFU mL^{-1} for both donor and recipient, [PI] = 1.0 mM, and the experiments were replicated three times with SD as the error bar).

concentrations (10^6, 10^7, and 10^8 CFU mL^{-1}) on *E. coli* strains HB101 and NK5449 inactivation by S-nZVI/PI are depicted in Fig. 5. It was observed that the viability of both donor and recipient decreased as their initial concentration increased. With initial donor and recipient concentrations set at 10^6, 10^7, and 10^8 CFU mL^{-1}, the inactivation efficiencies after 40 min reaction were 6.2, 5.0, and 3.8 $\log_{10}$ CFU mL^{-1} for the donor (Fig. 5a), and 6.1, 3.5, and 1.7 $\log_{10}$ CFU mL^{-1} for the recipient (Fig. 5b).

As shown in Fig. S3d, for the control group (without treatment with the S-nZVI/PI system), with initial donor and recipient concentrations set at 10^6, 10^7, and 10^8 CFU mL^{-1}, the numbers of transconjugants were 2.6, 3.8, and 5.0 $\log_{10}$ CFU mL^{-1} within 24 h of conjugative transfer, respectively, indicating that the density of bacteria played a vital role in the conjugative transfer of ARGs. Compared to the control group, after treatment with the S-nZVI/PI system, there was a decreasing trend in the number of transconjugants. The corresponding transconjugant numbers were 0 $\log_{10}$ CFU mL^{-1} for 10^6 CFU mL^{-1}, 1.1 $\log_{10}$ CFU mL^{-1} for 10^7 CFU mL^{-1}, and 2.9 $\log_{10}$ CFU mL^{-1} for 10^8 CFU mL^{-1} bacteria within 24 h. When the initial bacterial concentration was set to 10^6 CFU mL^{-1}, the donor and recipient were fully activated (Fig. 5). In addition, as shown in Fig. S3d, under this condition, as the mating time increased, part of *E. coli* NK5449 could recover its activity; however, there was no increase in *E. coli* HB101, thus resulting in 0 $\log_{10}$ CFU mL^{-1} of transconjugant.

The variation in the ARGs conjugative transfer frequency at different initial bacterial concentrations is shown in Fig. 6. When the initial concentrations of *E. coli* HB101 and *E. coli* NK5449 were 10^6, 10^7, and 10^8 CFU mL^{-1}, the conjugative transfer frequencies of ARGs were 0, 2.1×10^{-5}, and 6.6×10^{-5} within 24 h conjugative transfer after S-nZVI/PI system treatment, respectively, which were significantly lower than that of the corresponding control groups ($p < 0.05$). The results further revealed that the treatment of *E. coli* strains HB101 and NK5449 *via* the S-nZVI/PI system could impede the dissemination of ARGs *via* conjugation. Moreover, the results in Fig. 6 demonstrated that the efficiency of conjugative transfer increased with increasing initial concentration of bacteria in both the control and treatment groups ($p < 0.05$). As demonstrated in previous studies, the efficiency of horizontal gene transfer of ARGs was closely attributed to the concentrations of the donor and recipient.[38] When the concentration of bacteria was high, the interaction frequency of donor and recipient would increase, thus facilitating conjugative transfer.

3.1.4. Influence of interfering substances. The effect of interfering substances, such as HCO_3^-, NO_3^-, or HA, on the inactivation of *E. coli* HB101 and *E. coli* NK5449 by applying the S-nZVI/PI system is shown in Fig. 7. It was found that all investigated coexisting substances had a significant inhibitory effect on both investigated bacteria's inactivation ($p < 0.05$). After 40 min of treatment, the S-nZVI/PI system achieved bactericidal efficiencies of 3.8, 2.4, 3.5, and 3.4 $\log_{10}$ CFU mL^{-1} against *E. coli* HB101 (Fig. 7a), and 1.7, 0.8, 1.1, and 1.5 $\log_{10}$

© 2026 The Author(s). Published by the Royal Society of Chemistry

Open Access Article. Published on 02 March 2026. Downloaded on 5/24/2026 3:56:50 AM.
This article is licensed under a Creative Commons Attribution-NonCommercial 3.0 Unported Licence.

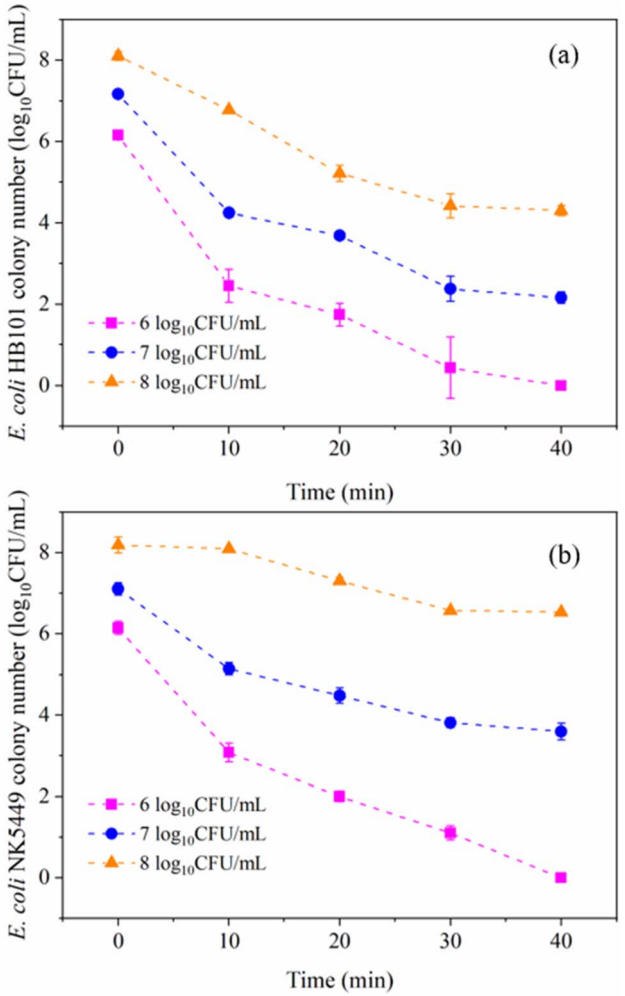

Fig. 5 Inactivation of (a) donor and (b) recipient as a function of the initial concentrations of donor and recipient. (Experimental conditions: $pH_0 = 6.8$, [S-nZVI] = 50 mg L^{-1}, [PI] = 1.0 mM, and the experiments were replicated three times with SD as the error bar).

CFU mL^{-1} against *E. coli* NK5449 (Fig. 7b) in blank (no interfering substance), HCO_3^-, NO_3^-, and HA-containing systems, respectively. HCO_3^- had the most serious adverse effect on the inactivation of bacteria among all the investigated coexisting substances. Previous studies demonstrated that $HO^\bullet$ and $O_2^{\bullet-}$ were responsible for inactivating *E. coli* HB101 in the S-nZVI/PI system,[25] which can be quenched by HCO_3^-;[39] as a result, the bactericidal performance of S-nZVI/PI decreased.

As depicted in Fig. S4a, when the mating time of donor and recipient was 3 h, compared to the blank group, there were transconjugants detected in HCO_3^-, NO_3^-, or HA containing systems; the corresponding number of transconjugants was 1.8 $\log_{10}$ CFU mL^{-1} for HCO_3^-, 1.4 $\log_{10}$ CFU mL^{-1} for NO_3^-, and 1.1 $\log_{10}$ CFU mL^{-1} for HA containing systems, illustrating that the existence of interfering substances could promote the generation of transconjugants. Moreover, the counts of the donor and recipient in interfering substances containing systems at 3 h of mating time were considerably greater than that of the blank system ($p < 0.05$) (Fig. S4a), thus promoting transconjugant generation. As the mating time increased to

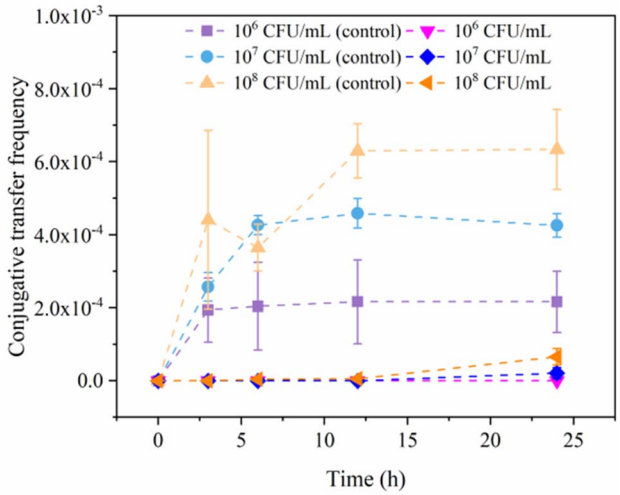

Fig. 6 Effect of the initial concentrations of donor and recipient on the ARGs conjugative transfer frequency. (Experimental conditions: $pH_0 = 6.8$, [S-nZVI] = 50 mg L^{-1}, [PI] = 1.0 mM, and the experiments were replicated three times with SD as the error bar).

24 h, all of the investigated groups appeared transconjugants, and the number of transconjugants showed no significant difference at different reaction systems ($p > 0.05$) (Fig. S4d).

The conjugative transfer frequencies of ARGs were 6.6×10^{-5}, 1.2×10^{-5}, 4.8×10^{-5}, and 2.3×10^{-5} for blank, HCO_3^-, NO_3^-, and HA containing systems within 24 h conjugative transfer after the S-nZVI/PI system treatment, respectively (Fig. 8). The presence of both HCO_3^- and HA significantly interfered with conjugative transfer ($p < 0.05$).

3.2. Influence mechanism of S-nZVI/PI on ARG conjugative transfer

3.2.1. Changes in intracellular LDH, ATP, and ROS levels. The levels of intracellular LDH, ATP, and ROS in the control (without S-nZVI/PI treatment) and S-nZVI/PI treatment groups are depicted in Fig. 9. Compared to the control group, the level of intracellular LDH of mixed donor and recipient bacteria remained unchanged after S-nZVI/PI treatment ($p > 0.05$) (Fig. 9a), indicating that the cell membrane was not destroyed during the disinfection process.[40] This was consistent with our previous study,[25] which showed that the cell membrane maintained its integrity after treatment with the S-nZVI/PI system, thus resulting in unchanged membrane permeability. This phenomenon indicated that the exchange of intracellular substances through pore channels could not be increased, which could not promote the ARGs conjugative transfer.[41] The level of ATP appeared a significant decreasing trend after treatment with S-nZVI/PI ($p < 0.05$). Specifically, when the donor and recipient bacteria were treated for 40 min, the level of ATP decreased by 0.4 μmol/10^6 cell against the control group (Fig. 9b). The conjugation transfer of ARGs is an energy-driven process that critically depends on ATP.[42] Hence, the decrease in ATP might be the dominant reason attributed to the decrease in ARGs conjugative transfer. Moreover, the intensity of ROS of the mixed donor and recipient bacteria after treatment with S-

Open Access Article. Published on 02 March 2026. Downloaded on 5/24/2026 3:56:50 AM.
This article is licensed under a Creative Commons Attribution-NonCommercial 3.0 Unported Licence.

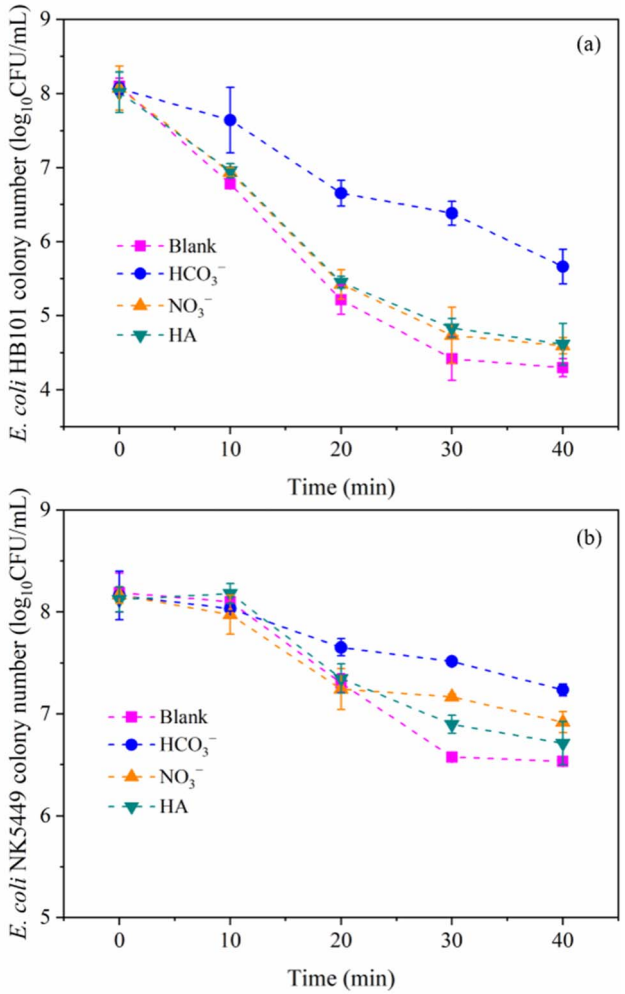

Fig. 7 Inactivation of (a) donor and (b) recipient in the presence of an interfering substance. (Experimental conditions: bacterial concentrations of 10^8 CFU mL^{-1} for both donor and recipient, $pH_0 = 6.8$, [S-nZVI] = 50 mg L^{-1}, [PI] = 1.0 mM, and the experiments were replicated three times with SD as the error bar).

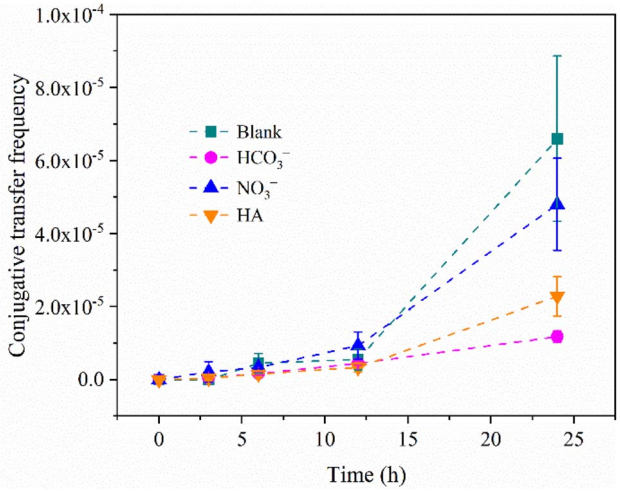

Fig. 8 Effect of the interfering substance on the ARGs conjugative transfer frequency. (Experimental conditions: bacterial concentrations of 10^8 CFU mL^{-1} for both donor and recipient, $pH_0 = 6.8$, [S-nZVI] = 50 mg L^{-1}, [PI] = 1.0 mM, and the experiments were replicated three times with SD as the error bar).

nZVI/PI was lower than that of the control group ($p < 0.05$) (Fig. 9c). These results might be due to the decrease in the numbers of donor and recipient bacteria after treatment with S-nZVI/PI (Fig. 1), which was in line with previous studies, as reported by Liu *et al.*[10] and Li *et al.*[43] As reported by Seaver *et al.*[44] and Imlay *et al.*,[45] ROS within bacteria were mainly produced during aerobic metabolism as inadvertent by-products. The treatment of donor and recipient bacteria by the S-nZVI/PI system disrupted the energy metabolism, which caused the bacterial respiratory chain function to cease and fundamentally cut off the source of ROS biosynthesis, thus resulting in a decrease in the ROS level.

3.2.2. Expression of different functional genes. To further investigate the influence mechanism of the S-nZVI/PI system on the conjugative transfer of ARGs, the expression of different functional genes after treatment with the S-nZVI/PI system was detected. As shown in Fig. 10, other than the *ompF* gene, compared to the control group, the expression of the genes, such as *flgC*, *trbA*, *traF*, *traG*, *traJ*, *korA*, *korB*, *rpoS*, *ompA*, and *ompC*, exhibited a decreasing trend after treatment with S-nZVI/PI ($p < 0.05$). The conjugative transfer of ARGs initiates with specific contact and pairing between donor and recipient bacteria. In this step, the donor bacterium expresses and extends sex pili, which recognizes and binds to the specific receptors on the surface of the recipient bacterium; then, the pili contract, thus causing the donor and recipient bacteria to adhere closely to each other. The *traF* gene participates in the assembly or stabilization of pili. After accomplishing the first process, the next procedure was to assemble a transmembrane DNA transport channel with the *trbA* gene acting as a key transcriptional repressor. Subsequently, the single-stranded DNA (ssDNA) in donor bacteria can be transferred to recipient bacteria through this channel, which is regulated by the *traG* gene. The final procedure is the replication of ssDNA in recipient bacteria. The ssDNA serves as a template for the synthesis of the complementary strand by the recipient's chromosomal replication system, which is then circularized to form a complete double-stranded plasmid. This process is dependent on the chromosome replication of the recipient bacteria rather than the plasmid genes. In addition to the aforementioned executing genes, the plasmid also contains some global regulation genes, such as *traJ*, *korA*, and *korB*, to realize global regulation during the ARGs conjugative transfer processes.[10,46] Moreover, the investigated *ompA*, *ompC*, and *ompF* genes express the outer membrane protein. The expression of the *ompF* gene is strictly regulated by applying the EnvZ/OmpR two-component system, and the activity of this system depends on the ATP-driven phosphorylation cascade reaction.[47] The fundamental reason for the elevation of the *OmpF* gene is most likely the inactivation of the key regulatory system (EnvZ/OmpR) due to energy depletion ATP. Combined with the LDH assay results, the downregulation of *ompA* and *ompC* and the

© 2026 The Author(s). Published by the Royal Society of Chemistry

Open Access Article. Published on 02 March 2026. Downloaded on 5/24/2026 3:56:50 AM.
This article is licensed under a Creative Commons Attribution-NonCommercial 3.0 Unported Licence.

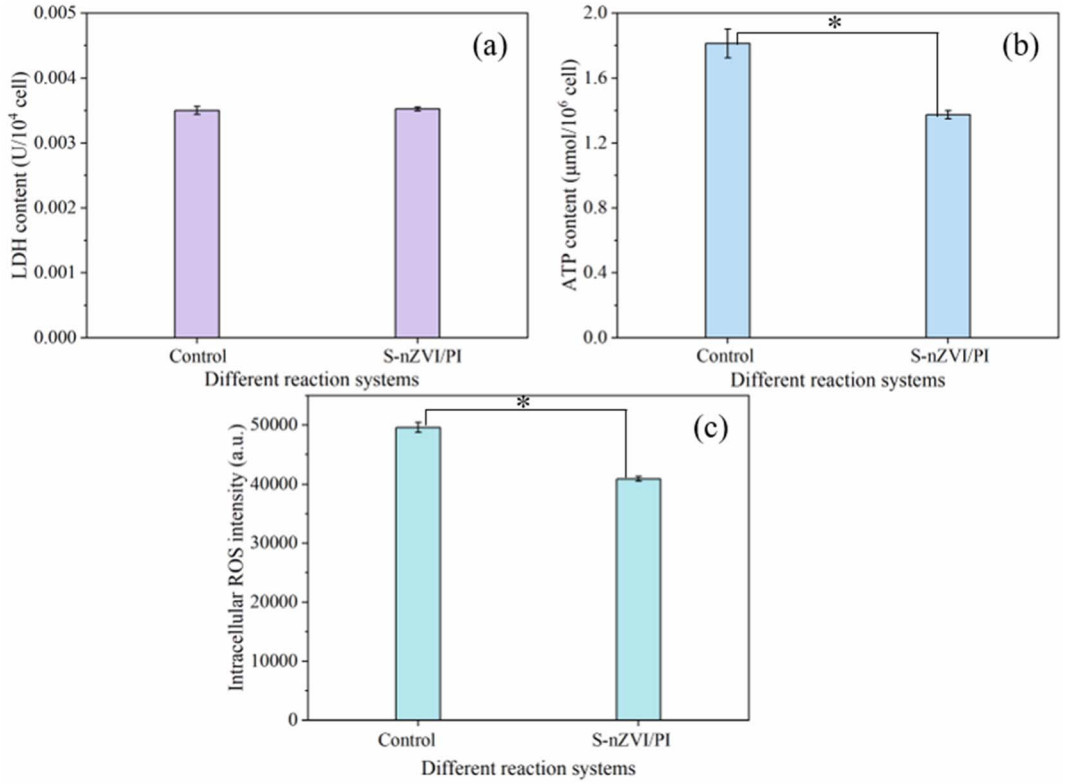

Fig. 9 Levels of (a) LDH, (b) ATP, and (c) ROS in the control and S-nZVI/PI-treated group after conjugative transfer. (Experimental conditions: [PI] = 1.0 mM, [S-nZVI] = 50 mg L^{-1}, bacterial concentrations of 10^8 CFU mL^{-1} for both donor and recipient, $pH_0 = 6.8$, the conjugative transfer time was 24 h, the experiments were replicated three times with SD as the error bar, and * indicates a significant difference, $p < 0.05$).

upregulation of *ompF* collectively determined that membrane permeability remained unchanged after S-nZVI/PI treatment. The downregulation of the *rpoS* gene might be associated with a decrease in ROS level after treatment with the S-nZVI/PI system.

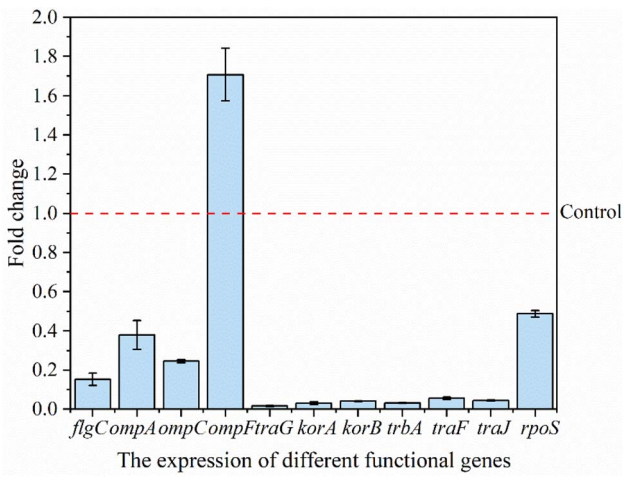

Fig. 10 Expression of different functional genes in the control and S-nZVI/PI-treated group after conjugative transfer. (Experimental conditions: PI = 1.0 mM, [S-nZVI] = 50 mg L^{-1}, bacterial concentrations of 10^8 CFU mL^{-1} for both donor and recipient, $pH_0 = 6.8$, the conjugative transfer time was 24 h, and the experiments were replicated three times with SD as the error bar).

Taken together, these findings indicate that the inhibiting efficacy of S-nZVI/PI treatment against ARGs conjugative transfer was predominantly ascribed to inhibiting the generation of ATP and downregulating some genes related to the contact and pairing (*traF*), the assembly of a transmembrane DNA transport channel (*trbA*), the transfer of ssDNA in donor bacteria to recipient bacteria (*traG*), and global regulation (*traJ*, *korA*, and *korB*).

4. Conclusions

In this study, the S-nZVI/PI system was utilized to inactivate the *E. coli* strains HB101 and NK5449 and investigate its impact on ARGs conjugative transfer under various conditions (such as different PI and S-nZVI dosages, initial bacterial concentrations, and interfering substances (such as HCO_3^-, NO_3^-, and HA)). The results of batch experiments demonstrated that an increase in the dosage of PI and S-nZVI had positive effects on the inactivation of the donor and recipient bacteria, whereas an increase in the initial concentrations of donor and recipient and the existence of interfering substances had negative effects. Moreover, ARGs conjugative transfer within 24 h increased with an increase in the initial bacterial concentration and decreased when the reaction of the S-nZVI/PI system contained HCO_3^- or HA. The mechanism of the inhibiting effect of the S-nZVI/PI system on ARGs conjugative transfer was ascribed to restraining the generation of ATP and the expression of some functional

Open Access Article. Published on 02 March 2026. Downloaded on 5/24/2026 3:56:50 AM. This article is licensed under a Creative Commons Attribution-NonCommercial 3.0 Unported Licence.

genes. This study only explored the inhibitory mechanism of ARGs conjugative transfer through indicators such as ATP, LDH, ROS, and a few functional genes, which have limitations in mechanism interpretation. In the future, multi-omics technologies (including transcriptome, proteome, and metabolome) should be used to systematically reveal the dynamic correlations among gene regulatory networks, functional protein execution, and cellular metabolic reprogramming during conjugative transfer to address the core limitations of previous studies in terms of mechanism systematicity. Moreover, direct characterization of the transient surface complex formed between S-nZVI and PI (*e.g.*, *via in situ* spectroscopic techniques or extended X-ray absorption fine structure) remains an important direction for future studies, which will provide the most definitive evidence for the atomic-scale mechanism of this system.

Author contributions

Li Liang: conceptualization, investigation, data curation, visualization, writing–original draft, writing–review & editing. Weiying Li: funding acquisition, supervision.

Conflicts of interest

The authors state that there are no conflicts of interest.

Data availability

All relevant data are provided within the article and its supplementary information (SI). Supplementary information is available. See DOI: https://doi.org/10.1039/d5ra08354k.

Acknowledgements

This research received support from the National Natural Science Foundation of China (No. 52470012) and the Science and Technology Plan Project of Jiaxing (No. 2024AY30015).

References

1 N. A. Sabri, H. Schmitt, B. Van Der Zaan, H. W. Gerritsen, T. Zuidema, H. H. M. Rijnaarts and A. A. M. Langenhoff, *J. Environ. Chem. Eng.*, 2020, **8**, 102245.
2 E. Szekeres, A. Baricz, C. M. Chiriac, A. Farkas, O. Opris, M. L. Soran, A. S. Andrei, K. Rudi, J. L. Balcázar, N. Dragos and C. Coman, *Environ. Pollut.*, 2017, **225**, 304–315.
3 L. Yang, Y. Shen, J. Jiang, X. Wang, D. Shao, M. M. C. Lam, K. E. Holt, B. Shao, C. Wu, J. Shen, T. R. Walsh, S. Schwarz, Y. Wang and Z. Shen, *Nat. Food*, 2022, **3**, 197–205.
4 S. Yao, J. Ye, Q. Yang, Y. Hu, T. Zhang, L. Jiang, S. Munezero, K. Lin and C. Cui, *Environ. Sci. Pollut. Res.*, 2021, **28**, 57321–57333.
5 Q. Q. Zhang, G. G. Ying, C. G. Pan, Y. S. Liu and J. L. Zhao, *Environ. Sci. Technol.*, 2015, **49**, 6772–6782.
6 Y. Ben, C. Fu, M. Hu, L. Liu, M. H. Wong and C. Zheng, *Environ. Res.*, 2019, **169**, 483–493.
7 S. Li, C. Zhang, F. Li, T. Hua, Q. Zhou and S. H. Ho, *J. Hazard. Mater.*, 2021, **411**, 125148.
8 B. Li, Y. Qiu, Y. Song, H. Lin and H. Yin, *Environ. Int.*, 2019, **131**, 105007.
9 Z. Qiu, Y. Yu, Z. Chen, M. Jin, D. Yang, Z. Zhao, J. Wang, Z. Shen, X. Wang, D. Qian, A. Huang, B. Zhang and J. W. Li, *Proc. Natl. Acad. Sci. U.S.A.*, 2012, **109**, 4944–4949.
10 Y. Liu, J. Gao, Y. Wang, W. Duan, Y. Zhang, H. Zhang and M. Zhao, *J. Hazard. Mater.*, 2022, **432**, 128722.
11 H. Gong, W. Chu, Y. Huang, L. Xu, M. Chen and M. Yan, *Environ. Pollut.*, 2021, **276**, 116691.
12 A. E. T. Anthony, M. O. Ojemaye, A. I. Okoh and O. O. Okoh, *J. Water Process Eng.*, 2021, **40**, 101919.
13 A. S. Ezeuko, M. O. Ojemaye, O. O. Okoh and A. I. Okoh, *J. Environ. Chem. Eng.*, 2021, **9**, 106183.
14 M. Herraiz-Carboné, S. Cotillas, E. Lacasa, C. Sainz De Baranda, E. Riquelme, P. Cañizares, M. A. Rodrigo and C. Sáez, *Sci. Total Environ.*, 2021, **797**, 149150.
15 M. Kalli, C. Noutsopoulos and D. Mamais, *Water*, 2023, **15**, 2084.
16 S. Li, B. S. Ondon, S. H. Ho, J. Jiang and F. Li, *Sci. Total Environ.*, 2022, **838**, 156544.
17 A. Pant, M. Shahadat, S. W. Ali and S. Z. Ahammad, *J. Hazard. Mater. Adv.*, 2022, **8**, 100189.
18 G. Zhang, W. Li, S. Chen, W. Zhou and J. Chen, *Chemosphere*, 2020, **254**, 126831.
19 M. T. Guo, Q. B. Yuan and J. Yang, *Environ. Sci. Technol.*, 2015, **49**, 5771–5778.
20 E. Sanganyado and W. Gwenzi, *Sci. Total Environ.*, 2019, **669**, 785–797.
21 R. Li, J. Wang, H. Zhu, Z. Guo and H. Zhu, *Sep. Purif. Technol.*, 2022, **292**, 120928.
22 L. Niu, K. Zhang, L. Jiang, M. Zhang and M. Feng, *J. Environ. Manage.*, 2022, **323**, 116241.
23 Y. Zong, Y. Shao, W. Ji, Y. Zeng, J. Xu, W. Liu, L. Xu and D. Wu, *Chem. Eng. J.*, 2023, **451**, 139106.
24 C. Ling, S. Wu, J. Han, T. Dong, C. Zhu, X. Li, L. Xu, Y. Zhang, M. Zhou and Y. Pan, *Water Res.*, 2022, **220**, 118676.
25 L. Liang, G. Zhang, X. Dai and W. Li, *Environ. Res.*, 2023, **236**, 116829.
26 Y. Zong, H. Zhang, Y. Shao, W. Ji, Y. Zeng, L. Xu and D. Wu, *J. Hazard. Mater.*, 2022, **423**, 126991.
27 F. Liu, Z. Li, Q. Dong, C. Nie, S. Wang, B. Zhang, P. Han and M. Tong, *Environ. Sci. Technol.*, 2022, **56**, 4413–4424.
28 K. Zhang, S. Zhang, C. Ye, R. Ou, H. Zeng, X. Yu and M. Feng, *Chem. Eng. J.*, 2023, **451**, 138642.
29 H. Sun, F. He and W. Choi, *Environ. Sci. Technol.*, 2020, **54**, 6427–6437.
30 F. Liu, Y. Hou, S. Wang, Z. Li, B. Zhang and M. Tong, *Water Res.*, 2023, **230**, 119508.
31 D. Fan, Y. Lan, P. G. Tratnyek, R. L. Johnson, J. Filip, D. M. O'Carroll, A. Nunez Garcia and A. Agrawal, *Environ. Sci. Technol.*, 2017, **51**, 13070–13085.
32 A. N. Garcia, Y. Zhang, S. Ghoshal, F. He and D. M. O'Carroll, *Environ. Sci. Technol.*, 2021, **55**, 8464–8483.
33 J. Guo, F. Gao, C. Zhang, S. Ahmad and J. Tang, *Chem. Eng. J.*, 2023, **477**, 147049.

© 2026 The Author(s). Published by the Royal Society of Chemistry

Open Access Article. Published on 02 March 2026. Downloaded on 5/24/2026 3:56:50 AM.
This article is licensed under a Creative Commons Attribution-NonCommercial 3.0 Unported Licence.

34 W. Xue, J. Li, X. Chen, H. Liu, S. Wen, X. Shi, J. Guo, Y. Gao, J. Xu and Y. Xu, *Environ. Sci. Pollut. Res.*, 2023, **30**, 101933–101962.
35 S. Yang, A. Liu, J. Liu, Z. Liu and W. Zhang, *Acta Chim. Sinica*, 2022, **80**, 1536.
36 L. Liang, X. Li, Y. Guo, Z. Lin, X. Su and B. Liu, *J. Hazard. Mater.*, 2021, **404**, 124057.
37 T. Zhang, Q. Gui, Y. Gao, M. Kong, S. Xu and Z. Wang, *Environ. Res.*, 2024, **252**, 118841.
38 Y. Su, D. Wu, H. Xia, C. Zhang, J. Shi, K. J. Wilkinson and B. Xie, *Environ. Int.*, 2019, **128**, 407–416.
39 G. Fang, J. Li, C. Zhang, F. Qin, H. Luo, C. Huang, D. Qin and Z. Ouyang, *Environ. Pollut.*, 2022, **300**, 118939.
40 J. Zhang, P. Su, H. Chen, M. Qiao, B. Yang and X. Zhao, *Chem. Eng. J.*, 2023, **451**, 138879.
41 Y. Zhou, G. Zhang, D. Zhang, N. Zhu, J. Bo, X. Meng, Y. Chen, H. Liu and W. Li, *Mar. Environ. Res.*, 2024, **202**, 106777.
42 K. Yu, F. Chen, L. Yue, Y. Luo, Z. Wang and B. Xing, *Environ. Sci. Technol.*, 2020, **54**, 10012–10021.
43 H. Li, Z. Kang, E. Jiang, R. Song, Y. Zhang, G. Qu, T. Wang, H. Jia and L. Zhu, *J. Hazard. Mater.*, 2021, **419**, 126465.
44 L. Seaver and J. Imlay, *J. Bacteriol.*, 2001, **183**, 7173–7181.
45 J. Imlay, *Annu. Rev. Biochem.*, 2008, **77**, 755–776.
46 R. Koebnik, K. P. Locher and P. Van Gelder, *Mol. Microbiol.*, 2000, **37**, 239–253.
47 X. Ji, A. Shi, J. Wang, B. Zhang, Y. Hu, H. Lv, J. Wu, Y. Sun, J.-M. Liu, Y. Zhang and S. Wang, *J. Agric. Food Chem.*, 2024, **72**, 18697–18707.

© 2026 The Author(s). Published by the Royal Society of Chemistry